

## Differential mobility and spatially heterogeneous dynamics of oxygen atoms in a supercooled glass-forming network liquid

Sabyasachi Sen

*Department of Chemical Engineering and Materials Science, University of California at Davis, Davis, California 95616, USA*

(Received 26 August 2008; published 19 September 2008)

Site-specific dynamics of oxygen atoms in a network silicate liquid (6.4%K<sub>2</sub>O-93.6%SiO<sub>2</sub>) has been studied in the glass transition region using high-temperature (up to 973 K) <sup>17</sup>O nuclear-magnetic-resonance spectroscopy. Chemical exchange between bridging and nonbridging oxygen environments is observed at a timescale that is orders of magnitude faster than that of shear relaxation. However, no significant self-exchange is observed at this timescale between the bridging oxygen environments. Implications of these results are discussed in relation to transport properties and glass transition in strong network liquids.

DOI: [10.1103/PhysRevB.78.100201](https://doi.org/10.1103/PhysRevB.78.100201)

PACS number(s): 61.43.Fs, 76.60.-k, 82.20.-w

The dynamical vs thermodynamic nature of the transition from glass to liquid has remained one of the important and controversial problems in solid-state physics.<sup>1,2</sup> A variety of complex phenomenological models has been proposed over the last several decades to explain the wide range of macroscopic dynamical phenomena in glass-forming liquids.<sup>3,4</sup> However, despite the sophisticated level of theory that has been developed to quantify these dynamical/relaxation processes, there is only a limited number of studies especially in the case of high-temperature network liquids where unambiguous mechanistic connections have been established at the atomic level.

The range of timescales associated with one- and two-dimensional exchange nuclear-magnetic-resonance (NMR) spectroscopy (approximately from microsecond to second) is ideally suited for probing a variety of site-specific atomic and molecular dynamical processes near glass transition.<sup>5-9</sup> Previous *in situ* high-temperature <sup>29</sup>Si and <sup>11</sup>B NMR spectroscopic studies have shown that in borate or silicate network liquids the average timescale of local Si-O or B-O bond breaking and chemical exchange between various Si or B species correspond well with the timescale of shear relaxation or viscous flow.<sup>7-9</sup> Taken together the results from these experiments indicate that the breaking and reforming of the network, i.e., of the bonds between network-forming cations and oxygen atoms control viscous flow in oxide network liquids. Therefore, the ability of oxygen atoms to explore various structural configurations should play a central role in controlling the transport and structural relaxation processes in network glass-forming oxide liquids. Unfortunately, such studies relating the dynamics of oxygen atoms to bulk transport and relaxation properties are completely lacking to date in the literature. For example, exchange between bridging oxygen atoms (BOs) bonded to two network-forming cations and nonbridging oxygen atoms (NBOs) bonded to one network-forming cation does not require concomitant exchange of various cationic species. Hence, the two processes can be decoupled at least at low temperatures near glass transition. On the other hand, oxygen atoms in NBO and BO configurations may have different mobility, i.e., cross-exchange between BO and NBO may occur at a different rate than the self-exchange between them. Moreover, such differences may be more pronounced in networks with

high degree of connectivity such that the concentration of NBOs is not high enough to percolate through the system and statistical separation between NBOs is large. This scenario would indicate existence of strong dynamical heterogeneities even in strong network liquids especially at low temperatures near glass transition. The presence of dynamical heterogeneities has so far been confirmed only in the case of fragile ionic, molecular, and polymeric liquids.<sup>10-14</sup> Their existence in strong network liquids may have important implications in our understanding of the nature of potential-energy landscapes of these liquids and of glass transition phenomena in general.

We report here the results of a high-temperature and high-resolution <sup>17</sup>O magic-angle-spinning nuclear-magnetic-resonance (MAS NMR) study of oxygen dynamics in a supercooled binary potassium silicate (6.4 mol % K<sub>2</sub>O-93.6 mol % SiO<sub>2</sub>) glass-forming liquid (glass transition temperature  $T_g \sim 848$  K) with a structure characterized by a small concentration of NBOs and, therefore, a high degree of connectivity of the Si-O network. The glass sample was prepared from K<sub>2</sub>CO<sub>3</sub> and <sup>17</sup>O-enriched SiO<sub>2</sub> reagents in Pt-Rh crucibles by conventional melt quenching method in a flowing Ar atmosphere. Details of the sample preparation and chemical characterization can be found elsewhere.<sup>15</sup> All <sup>17</sup>O MAS NMR spectra reported here were collected at a Larmor frequency of 67.75 MHz (11.7 T) using a Bruker wide-bore magnet and a Bruker Avance 500 solid-state NMR spectrometer. A high-resolution <sup>17</sup>O MAS NMR spectrum was collected at ambient temperature using a Bruker cross-polarization MAS (CPMAS) probe. Crushed glass was loaded into 2.5 mm zirconia rotors for sample spinning at 22 to 23 kHz and the spectrum was collected with 0.6 μs excitation pulses ( $< \pi/4$ ), 1 s recycle delays, and signal averaging of 5000 scans. The variable-temperature <sup>17</sup>O MAS NMR spectra of the glass and the supercooled liquid were collected over temperatures ranging between ambient and 973 K using a high-temperature MAS probe (Doty Inc.). The crushed glass was taken in a boron nitride capsule that was inserted into a Si<sub>3</sub>N<sub>4</sub> rotor and was spun at speeds ranging between 6.0 and 6.6 kHz. The <sup>17</sup>O MAS NMR spectra were collected with 1 μs excitation pulses ( $< \pi/4$ ), 5 s recycle delays, and signal averaging of 100 scans. All <sup>17</sup>O MAS NMR data were referenced to <sup>17</sup>O-labeled H<sub>2</sub>O.

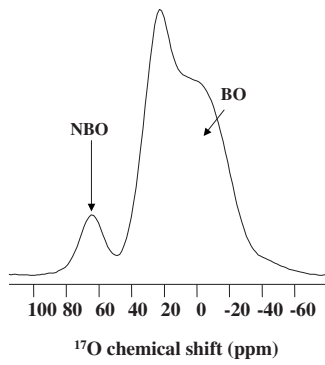


FIG. 1. High-resolution  $^{17}\text{O}$  MAS NMR spectrum of the K-silicate glass collected at ambient temperature. Peaks corresponding to NBO and BO are as shown. Spinning sidebands are outside the spectral region shown here.

The high-resolution central transition ( $\frac{1}{2} \leftrightarrow -\frac{1}{2}$ )  $^{17}\text{O}$  MAS NMR spectrum shows clear resolution of the BO and NBO sites (Fig. 1). The narrow nearly Gaussian peak centered at  $\sim 60$  ppm corresponds to the NBO sites while the broad quadrupolar line shape in the spectrum (+40 to  $-40$  ppm) corresponds to the BO sites (Fig. 1).<sup>16,17</sup> The concentration of NBOs in this glass can be easily obtained by integrating the areas under the BO and NBO peaks in the  $^{17}\text{O}$  MAS

NMR spectrum. Such calculation show that in this glass  $\sim 6.5\%$  of all the oxygen atoms are present as NBOs, in good agreement with the theoretically expected value of  $\sim 6.6\%$ .

The variable-temperature  $^{17}\text{O}$  MAS NMR spectra collected at a slower spinning speed contain spinning sidebands; however, they clearly distinguish the BO and NBO signals for the glass and the supercooled liquid [Fig. 2(a)]. The ambient temperature  $^{17}\text{O}$  MAS NMR spectrum does not show any significant change upon increasing the temperature to up to 823 K except some deshielding ( $\sim 5$  ppm) of the BO chemical shift that results in a stronger overlap of the BO and NBO peaks with increasing temperature [Fig. 2(a)]. Previous *ab initio* calculations of the  $^{17}\text{O}$   $\delta_{\text{iso}}$  for BOs in Si-O-Si linkages have shown that it is negatively correlated with both Si-O-Si angle and Si-O distance.<sup>17</sup> Thus the observed deshielding of the  $^{17}\text{O}$  MAS NMR signal in Fig. 2(a) can readily be attributed to the thermal expansion of the Si-O network and concomitant increase in the Si-BO distance in the glass. In contrast, the  $^{17}\text{O}$  MAS NMR line shape shows significant changes at and above 873 K. At  $973 \geq T \geq 873$  K the intensity of the NBO peak decreases while it starts merging with the BO peak indicating chemical exchange between BO and NBO sites [Fig. 2(a)].

These temperature-induced changes in the experimental  $^{17}\text{O}$  MAS NMR line shapes have been simulated using random multisite exchange models. Simulation of dynamically

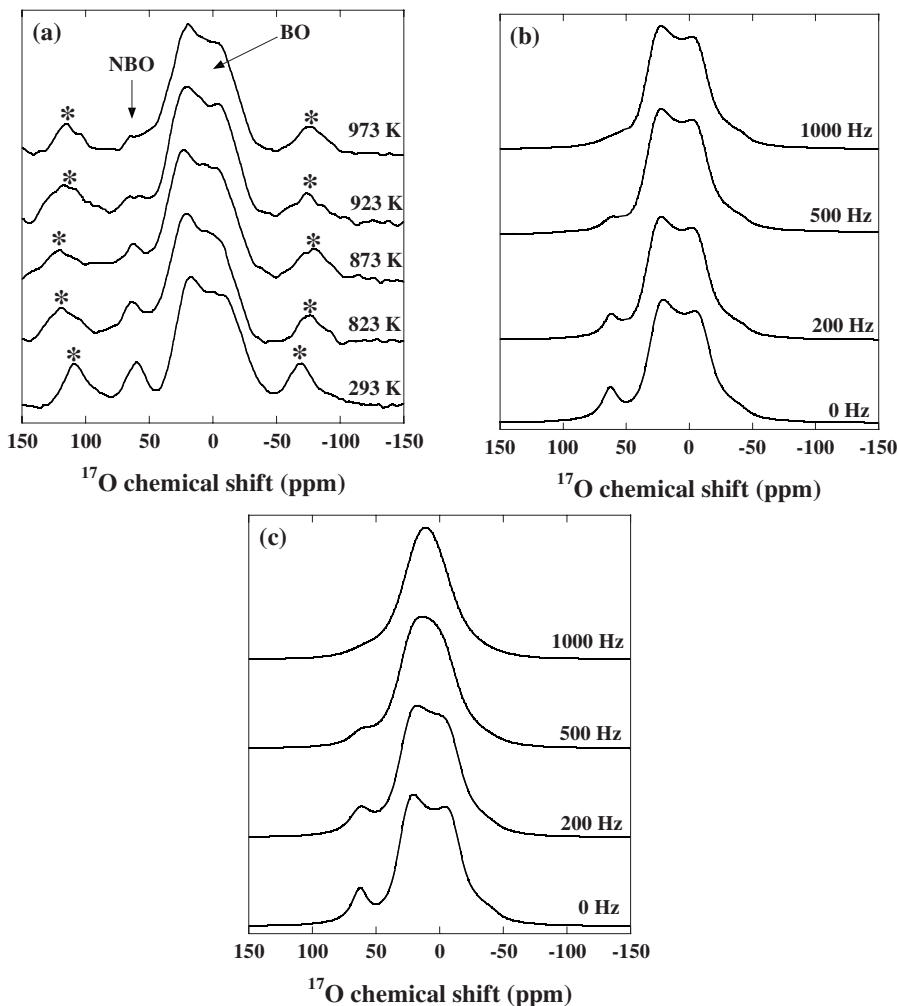


FIG. 2. (a) Experimental  $^{17}\text{O}$  MAS NMR spectra of the K-silicate glass and supercooled liquid collected at different temperatures. Temperatures are indicated alongside each spectrum. Asterisks denote spinning sidebands in the experimental spectra. Note the effect of BO-NBO cross-exchange on the NBO line shapes with increasing temperature and exchange frequency. (b) Simulated  $^{17}\text{O}$  MAS NMR spectra as a function of increasing (from bottom to top) rates of BO-NBO cross-exchange without any self-exchange between BO sites. Corresponding exchange frequencies are indicated alongside each spectrum. See text for details of the simulation procedure. (c) Simulated  $^{17}\text{O}$  MAS NMR spectra as a function of increasing (from bottom to top) rates of self- and cross-exchange between all oxygen sites. Corresponding exchange frequencies are indicated alongside each spectrum. See text for details of the simulation procedure.

modulated NMR line shapes dominated by quadrupolar effect involves deconvolution of the “rigid-lattice” spectrum into equally spaced Gaussian or Lorentzian components representing sites with different orientations of the electric-field-gradient (EFG) tensor with respect to the magnetic field. The  $^{17}\text{O}$  MAS NMR spectrum obtained at 823 K has been used to represent the rigid-lattice spectrum with no detectable exchange between oxygen sites. This  $^{17}\text{O}$  MAS NMR spectrum can be simulated well with a second-order quadrupolar broadened line shape for the BO sites with isotropic chemical shift  $\delta_{\text{iso}} \sim 40$  ppm, quadrupolar coupling constant  $Cq = 5.02 \pm 0.10$  MHz, and asymmetry parameter  $\eta = 0.20 \pm 0.05$  and a Gaussian line shape for the NBO sites with  $\delta_{\text{iso}} \sim 63$  ppm [Fig. 2(a)]. These  $Cq$  and  $\eta$  values are consistent with those observed for BO sites in vitreous  $\text{SiO}_2$ .<sup>17</sup> Approximately 40 000 sites have been used to simulate this second-order quadrupolar broadened central transition  $^{17}\text{O}$  MAS NMR line shape with a site exchange frequency of zero [Fig. 2]. The analytical expression for the resulting line shape is given by the real part of  $g(\omega)$ , where  $g(\omega) = 1/N[L/(1 - (L/\tau_{\text{NMR}}))]^2$  and  $L = \sum_{j=1,N} [i(\omega - \omega_j) + 1/T_{2j} + N/\tau_{\text{NMR}}]^{-1}$ .  $N$  is the total number of sites with different orientations  $j$  of the EFG tensor,  $\omega_j$  is the frequency and  $T_{2j}$  is the reciprocal of the intrinsic linewidth corresponding to the orientation  $j$ , and  $(\tau_{\text{NMR}})^{-1}$  is the frequency of random exchange between the different orientations.<sup>18</sup> The value of  $T_{2j}$  has been kept constant as 2 ms for all orientations in all of the simulations and only  $(\tau_{\text{NMR}})^{-1}$  is varied as a function of temperature to simulate the  $^{17}\text{O}$  MAS NMR spectra in the temperature range  $973 \geq T \geq 873$  K. Any effect of thermal expansion on  $^{17}\text{O}$  NMR chemical shift is assumed to be negligible in this temperature range. The effects of spinning sidebands and quadrupolar satellite transitions have been ignored in these simulations. This approach should be rigorously valid since the exchange frequencies considered here ( $\leq 1$  kHz) are significantly slower than the spinning rate ( $\sim 6$  kHz) and several orders of magnitude smaller than the widths of the quadrupolar satellite peaks.

Two different models of random multisite exchange have been used for these simulations. The  $^{17}\text{O}$  MAS NMR line shapes in Fig. 2(b) represent an exchange model where only cross-exchange between NBO and BO sites is considered and no self-exchange between BO sites with different orientations are allowed. In contrast, the corresponding line shapes in Fig. 2(c) correspond to an exchange model where self-exchange is possible between BO sites with all possible local orientations in addition to cross-exchange between them and the NBO site. A single mean-exchange frequency  $(\tau_{\text{NMR}})^{-1}$  is used for both self- and cross-exchange events. A comparison between the experimental and simulated  $^{17}\text{O}$  MAS NMR line shapes in Fig. 2 clearly indicates that the experimental line shapes are consistent with the absence of any detectable self-exchange between the BO sites. The experimental line shapes at 873, 923, and 973 K can be simulated well with cross-exchange between NBO and BO sites at frequencies  $(\tau_{\text{NMR}})^{-1}$  of 200, 500, and 1000 Hz, respectively [Fig. 2(b)]. The time scale  $\tau_{\text{NMR}}$  of BO-NBO cross-exchange is compared with that of the macroscopic shear relaxation process  $\tau_{\text{shear}}$  derived from the viscosity data in an Arrhenius plot in Fig. 3. The activation energy of BO-NBO

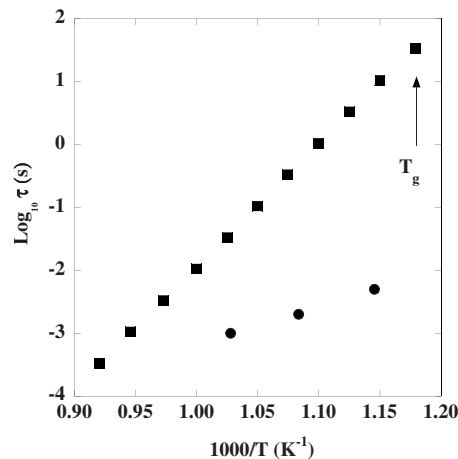


FIG. 3. Comparison between  $\tau_{\text{NMR}}$  (circles) and  $\tau_{\text{shear}}$  (squares) for the K-silicate glass and supercooled liquid at different temperatures. The average shear relaxation times  $\tau_{\text{shear}}$  at temperatures  $T \geq T_g$  has been calculated from the shear viscosities  $\eta$  of the supercooled liquid (determined by standard beam-bending method) using the Maxwell relation  $\tau_{\text{shear}} = \eta/G_\infty$  where  $G_\infty$  represents the infinite frequency shear modulus which is nearly independent of temperature and can be treated as a constant  $\sim 3 \times 10^{10}$  Pa for a wide variety of silicate glass formers (Ref. 3). The arrow pointing upward marks  $T_g$ .

cross-exchange ( $\sim 114 \pm 12$  kJ mol<sup>-1</sup>) is substantially lower than that of viscous flow ( $\sim 370$  kJ mol<sup>-1</sup>). Thus, the timescales for viscous flow and shear relaxation processes appear to be strongly decoupled from that of the cross-exchange between NBO and BO sites in this glass with high  $\text{SiO}_2$  content. The spectroscopic data also indicate that over the time scale associated with BO-NBO cross-exchange, a large fraction of BO sites are immobile and only those BO sites that locally exchange with the NBO sites are taking part in diffusive transport of oxygen. Since nearly 90% of the oxygen atoms are present as BO, the lack of self-exchange between the BO sites implies highly spatially heterogeneous oxygen dynamics in this temperature range near glass transition. The regions or domains of “high” oxygen mobility, characterized by BO-NBO cross-exchange, are expected to be embedded in a BO-rich matrix characterized by “low” oxygen mobility. The regions of high oxygen mobility would be rare and disconnected at any instant simply due to the small concentration of NBO sites in the structure. However, such regions may dynamically percolate over time through BO-NBO exchange giving rise to long-range diffusive transport of oxygen and global structural relaxation. Therefore, in this scenario, the glass transition is controlled by the temperature and time dependence of this dynamical percolation process.

The direct observation of strong differential mobility of fast NBO and slow BO sites (except for those BO that are involved in cross-exchange with the NBO) in this study may have far-reaching implications in understanding the transport properties of oxide network glass-forming liquids. For example, progressive increase in the relative fraction of mobile NBO sites is expected to lead to a rapid increase in the diffusivity of network-forming ions, and a corresponding drop

in the viscosity of silicate liquids until an infinitely percolating cluster of NBO sites is established in the structure at some critical NBO concentration. Such a critical transition in the compositional dependence of the transport properties has indeed been observed in a wide variety of silicate liquids at NBO fractions of  $\sim 16\%$  of all oxygen atoms.<sup>19</sup> On the other hand, recent comprehensive analyses of the diffusion processes in vitreous silica have conclusively indicated that oxygen diffusivity is significantly faster than the diffusivity of Si atoms and only the latter is strongly coupled to the viscosity and crystal-growth rate over temperatures ranging between  $T_g$  and melting point.<sup>20–22</sup> Oxygen diffusivity in vitreous  $\text{SiO}_2$  is characterized by a lower activation energy of  $\sim 100\text{--}300\text{ kJ mol}^{-1}$  (depending on the impurity concentration) compared to the activation energies for Si diffusion, viscosity, and crystal growth ( $550\text{--}590\text{ kJ mol}^{-1}$ ) indicating strong decoupling between Si and O motion.<sup>20,21</sup> It has been speculated that the unavoidable presence of small concentration of NBO atoms due to impurities in vitreous  $\text{SiO}_2$  is possibly responsible for the faster diffusion pathways for oxygen.<sup>20,21</sup> The validity of this speculation rests on the existence of differential mobility of NBO and BO species that can be experimentally verified directly only with  $^{17}\text{O}$  NMR spectroscopy. Hence, in this study, the observation of such differential mobility and fast hopping of NBO species with an activation energy of  $\sim 114\text{ kJ mol}^{-1}$  in a high- $\text{SiO}_2$  glass provide direct experimental support to this hypothesis. Moreover, the results reported here also shed light on another important transport-related problem in network glasses, namely, the nature of the diffusion or ionic conduction pathway at low temperatures ( $T \leq T_g$ ) for network-modifying cations in glasses with low modifier concentrations below percolation threshold. In this situation the statistical separation between modifier ions can be so large (e.g.,  $5\text{ \AA}$  or more)

that cooperative hopping between modifier sites becomes impossible without rearrangement of the network. However, the timescale of structural rearrangement of the network is expected to be much longer than the hopping timescale of the modifier ions, especially at  $T \leq T_g$ , thus excluding the possibility of any coupling between modifier ion conduction and network relaxation. The results of this study, on the other hand, indicate that in alkali silicate glasses with low alkali concentrations the relatively fast local exchange between NBO and BO sites (compared to network structural relaxation timescale) may provide dynamically percolating pathways for concomitant hopping of alkalis. This scenario is consistent with fact that the activation energies for alkali diffusion ( $\sim 90\text{--}100\text{ kJ mol}^{-1}$ )<sup>23</sup> in glasses of similar composition are indeed similar to that observed in this study for NBO-BO cross-exchange. It is further consistent with the results of recent molecular-dynamics studies of silicate glasses with low alkali content that have indeed shown that in such systems the mobility of alkali ions critically depends on the presence of NBO in their nearest-neighbor coordination environment.<sup>24</sup>

In summary, direct spectroscopic evidence is found for strong differential mobility of BO and NBO sites and consequently for spatial dynamical heterogeneity in the network of a supercooled silicate liquid near glass transition. The timescale of NBO-BO cross-exchange is found to be orders of magnitude faster and to have an activation energy that is a factor of 3 lower than those characteristic of the shear relaxation process. These results may play a key role in our understanding of transport processes associated with glass transition and ionic conduction in strong network liquid

This work was supported by NSF under Grant No. DMR-0603933.

- 
- <sup>1</sup>J. C. Dyre, *Rev. Mod. Phys.* **78**, 953 (2006).  
<sup>2</sup>V. Lubchenko and P. G. Wolynes, *Annu. Rev. Phys. Chem.* **58**, 235 (2007).  
<sup>3</sup>G. N. Greaves and S. Sen, *Adv. Phys.* **56**, 1 (2007).  
<sup>4</sup>C. A. Angell, K. L. Ngai, G. B. McKenna, P. F. McMillan, and S. W. Martin, *J. Appl. Phys.* **88**, 3113 (2000).  
<sup>5</sup>K. Schmidt-Rohr and H. W. Spiess, *Multidimensional Solid-State NMR and Polymers* (Academic, New York, 1994).  
<sup>6</sup>E. L. Gjersing, S. Sen, P. Yu, and B. G. Aitken, *Phys. Rev. B* **76**, 214202 (2007).  
<sup>7</sup>I. Farnan and J. F. Stebbins, *Science* **265**, 1206 (1994).  
<sup>8</sup>J. F. Stebbins and S. Sen, in *Borate Glasses, Crystals and Melts*, edited by A. C. Wright, S. A. Feller, and A. C. Hannon (Society of Glass Technology, Sheffield, UK, 1997), pp. 34–41.  
<sup>9</sup>J. F. Stebbins and S. Sen, *J. Non-Cryst. Solids* **224**, 80 (1998).  
<sup>10</sup>S. Sen and J. F. Stebbins, *Phys. Rev. Lett.* **78**, 3495 (1997).  
<sup>11</sup>S. F. Swallen, P. A. Bonvallet, R. J. McMahon, and M. D. Ediger, *Phys. Rev. Lett.* **90**, 015901 (2003).  
<sup>12</sup>M. K. Mapes, S. F. Swallen, and M. D. Ediger, *J. Phys. Chem. B* **110**, 507 (2006).  
<sup>13</sup>X. Qiu and M. D. Ediger, *J. Phys. Chem. B* **107**, 459 (2003).  
<sup>14</sup>S. A. Reinsberg, A. Heuer, B. Doliwa, H. Zimmermann, and H. W. Spiess, *J. Non-Cryst. Solids* **307-310**, 208 (2002).  
<sup>15</sup>S. Sen and R. E. Youngman, *J. Non-Cryst. Solids* **331**, 100 (2003).  
<sup>16</sup>S. E. Ashbrook and M. E. Smith, *Chem. Soc. Rev.* **35**, 718 (2006); J. F. Stebbins, J. V. Oglesby, and S. K. Lee, *Chem. Geol.* **174**, 63 (2001).  
<sup>17</sup>T. M. Clark, P. J. Grandinetti, P. Florian, and J. F. Stebbins, *Phys. Rev. B* **70**, 064202 (2004).  
<sup>18</sup>M. Mehring, *Principles of High Resolution NMR in Solids* (Springer-Verlag, Berlin, 1983).  
<sup>19</sup>S. Sen and T. Mukerji, *Geophys. Res. Lett.* **24**, 1015 (1997).  
<sup>20</sup>Marcio Luis Ferreira Nascimento and E. D. Zanotto, *Phys. Rev. B* **73**, 024209 (2006).  
<sup>21</sup>M. L. F. Nascimento and E. D. Zanotto, *Phys. Chem. Glasses* **48**, 201 (2007).  
<sup>22</sup>A. Saksengwijit and A. Heuer, *Phys. Rev. E* **74**, 051502 (2006).  
<sup>23</sup>N. P. Bansal and R. H. Doremus, *Handbook of Glass Properties* (Academic, Orlando, 1986).  
<sup>24</sup>A. N. Cormack, J. Du, and T. R. Zeitler, *J. Non-Cryst. Solids* **323**, 147 (2003).